RSC Advances

PAPER

View Article Online
View Journal | View Issue

Cite this: *RSC Adv.*, 2016, **6**, 10750

Stepwise synthesis of mixed-metal assemblies using pre-formed Ru(II) 'complex ligands' as building blocks†

Alexander J. Metherell and Michael D. Ward*

Two families of heteronuclear coordination complexes have been prepared in a stepwise manner using pre-formed, kinetically inert $[RuL_3]^{2+}$ building blocks, in which L is a bis-bidentate bridging ligand with two pyrazole–pyridyl termini, coordinated at one end to the Ru(II) centre. These pre-formed 'complex ligands' – with three pendant binding sites – react with additional labile transition metal dications to complete the stepwise assembly of mixed-metal arrays in which labile [Co(II)/Cd(II)] or inert [Ru(II)] ions strictly alternate around the framework. When L = the thiophene-2,5-diyl spaced ligand L^{th}, the complex $[Ru(L^{th})_3]^{2+}$ is formed in the expected 3 : 1 *mer* : *fac* ratio: reaction with labile Co(II) or Cd(II) ions completes formation of a heteronuclear square $[Ru_2Co_2(L^{th})_6]^{8+}$ or one-dimensional coordination polymer $\{[CdRu(L^{th})_3]^{4+}\}_\infty$, respectively. In these only the *mer* isomer of $[Ru(L^{th})_3]^{2+}$ is selected by the self-assembly process, whereas the *fac* isomer is not used. When L = a 1,3-benzene-diyl spaced ligand (L^{ph}), the complex ligand $[Ru(L^{ph})_3]^{2+}$ formed in the initial step is enriched in *mer* isomer (80–87% *mer*, depending on reaction conditions). Two quite different products were isolated from reaction of $[Ru(L^{ph})_3]^{2+}$ with Co(II) depending on the conditions. These are the rectangular, hexanuclear 'open-book' array $[Ru_3Co_3(L^{ph})_9]^{12+}$ which contains a 2 : 1 proportion of *fac*/*mer* Ru(II) metal centres; and the octanuclear cubic $[Ru_4Co_4(L^{ph})_{12}\{Na(BF_4)_4\}]^{13+}$ cage which is a new structural type containing all *mer* Ru(II) vertices and all *fac* Co(II) vertices. The cavity of this cubic cage contains a tetrahedral array of fluoroborate anions which in turn coordinate to a central Na(I) ion – an unusual example of a metal complex $[Na(BF_4)_4]^{3-}$ acting as the guest inside the cage-like metal complex $[Ru_4Co_4(L^{ph})_{12}]^{16+}$.

Received 29th October 2015
Accepted 11th January 2016

DOI: 10.1039/c5ra22694e

www.rsc.org/advances

Introduction

Polynuclear coordination cages – hollow, pseudo-spherical metal/ligand capsules – are a field of major importance within supramolecular chemistry.[1] Originally interest in them arose because of the possibility of making elaborate new structures from simple components by self-assembly methods. With this starting to become a mature field, the focus is now shifting towards the functional behaviour that can arise when guests bind in the central cavity.[2–5] The vast majority of coordination cages – even those with very elaborate structures – are based on just two types of component, *i.e.* one type of metal ion and one type of bridging ligand.[1] Whilst this is not important if the cage is acting simply as a container with a central cavity having a particular size, shape and other physical characteristics, it is limiting if one wishes to introduce additional functionality *via* the metal centres such as redox activity, magnetism, colour or luminescence: examples of cages where these characteristics are important are surprisingly limited.[5]

We have recently been interested to include metal ions such as Ru(II) and Os(II) into coordination cage assemblies to exploit their well known redox and luminescence properties in coordination cages that consequently have a wider range of useful properties than simply the ability to bind guests.[6] The reversible redox behaviour of these at modest potentials,[6a,b] and the availability of stable, long-lived MLCT excited states of an array of chromophores around the central cavity,[6b] make these particularly appealing metal ions which could allow (for example) a reversible change in the charge of a host cage, or the ability to effect photoinduced energy/electron transfer to a bound guest. However, these desirable properties are also associated with the high kinetic inertness of second- and third-row transition metal ions in a low-spin configuration, which makes Ru(II) and Os(II) very difficult to use in conventional self-assembly processes which rely on kinetic lability.

The consequence of this is that a more sophisticated synthetic strategy must be used to permit inclusion of kinetically inert metal ions in elaborate self-assembled polynuclear metal assemblies. The strategy is a stepwise 'complexes as ligands' approach that we[6] and others[7] have used. This involves

Department of Chemistry, University of Sheffield, Sheffield S3 7HF, UK. E-mail: m.d.ward@sheffield.ac.uk

† Electronic supplementary information (ESI) available. CCDC 1433701–1433703. For ESI and crystallographic data in CIF or other electronic format see DOI: 10.1039/c5ra22694e

initial preparation of a mononuclear complex of the kinetically inert metal ion but which bears pendant binding sites at which cage assembly can propagate. Combination of this 'complex ligand' with labile ions in a separate step results in completion of the cage assembly in which, necessarily, the labile and inert metal ions strictly alternate around the periphery. This is notably different from the use of unsymmetrical ligands, which possess both hard and soft binding sites which will selectively bind to hard and soft metals, respectively: this has been exploited by many groups to give mixed-metal cage assemblies but this method still requires both types of metal to be labile.[8]

Our recent efforts towards this end have focussed on the preparation of heterometallic $[(M^a)_4(M^b)_4(L^{naph})_{12}]X_{16}$ cubic coordination cages (where M^a = Os/Ru, and M^b = Co/Cd; see Scheme 1 for ligand structure); these were prepared from inert $[(M^a)(L^{naph})_3]^{2+}$ 'complex ligands' with three pendant binding sites arising from the ditopic ligands, by reaction with additional labile $[M^b]^{2+}$ ions (Fig. 1).[6a,b] These structures are essentially the same as those of the homonuclear $[M_8(L^{naph})_{12}]X_{16}$ parent cages, in which eight octahedral metals define the vertices of an approximate cube, and twelve bis-bidentate bridging ligands define the edges.[9] Both Ru(II) and Os(II) impart redox activity to the cages, allowing the charge on the cage cation to be switched reversibly between 16+ and 20+. In addition the Os(II) tris(pyrazolyl-pyridine) units have a long-lived excited state which is good electron-donor, potentially allowing photoinduced electron transfer from the cage superstructure to bound guests.[6b]

A subtle but crucial structural feature which allowed the stepwise assembles of these heterometallic cages to work is the geometric isomerism of the metal vertices.[6b,7i] These $[M_8(L^{naph})_{12}]X_{16}$ cages possess two facial (*fac*) tris-chelate metal sites at opposite corners of a long diagonal of the cube. The six remaining metals all possess a meridional (*mer*) tris-chelate coordination geometry, such that the cages have overall molecular S_6 symmetry. This particular combination of *fac* and *mer* metal centres arises spontaneously in the self assembly of these particular cages when labile metal ions such as Co(II) are used[9] (in other types of cage this ratio may be different according to the requirements of each cage structure).[1c] Fortuitously, this 1 : 3 ratio of *fac* : *mer* metal complex units is also exactly what arises for simple statistical reasons when the mononuclear $[(M^a)(L^{naph})_3]^{2+}$ 'complex ligands' are prepared using Ru(II) or Os(II). This means that we can prepare mononuclear $[(M^a)(L^{naph})_3]^{2+}$ (M^a = Ru, Os) and use the 1 : 3 *fac* : *mer* mixture of geometric isomers directly, without separation, to complete the assembly of the heterometallic $[(M^a)_4(M^b)_4(L^{naph})_{12}]X_{16}$ cages which, precisely, require one of the four M^a sites to be *fac* and the other three to be *mer*.[6a,b]

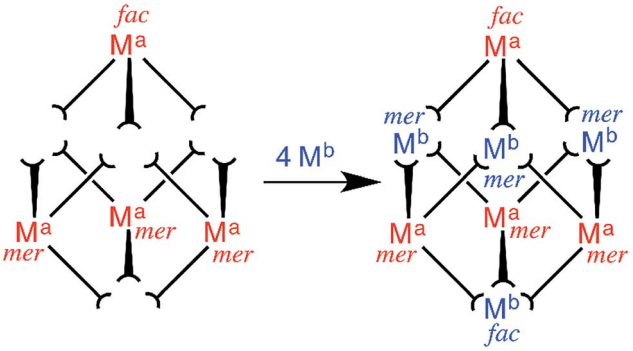

Fig. 1 Sketch outlining the stepwise synthetic strategy used to prepare the heterometallic cubic cage complexes: *viz* combination of pre-formed, kinetically inert $[(M^a)(L^{naph})_3]^{2+}$ (M^a = Ru, Os) units with additional labile ions $(M^b)^{2+}$ (M^b = Co, Cd) in a 4 : 4 ratio to give octanuclear $[(M^a)_4(M^b)_4(L^{naph})_{12}]^{16+}$.[6a,b]

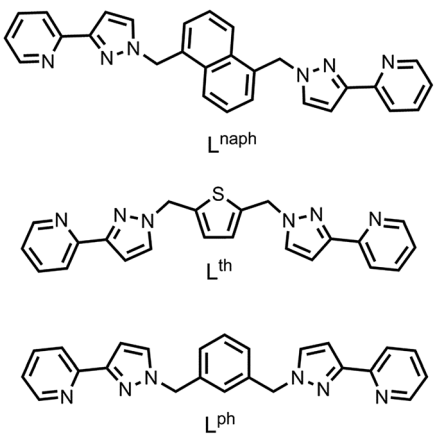

Scheme 1 Structures of the ligands discussed in this work.

In this contribution, we look at heterometallic assemblies containing Ru(II) ions as the inert component but based on different bridging ligands (L^{ph} and L^{th}, with 1,3-benzene-diyl and thiophene-2,5-diyl spacers separating the two pyrazolyl-pyridine termini – see Scheme 1). These ligands have afforded some new heterometallic assemblies whose formation is controlled by the availability of different proportions of *fac* and *mer* mononuclear units, and include an unusual new type of heterometallic cubic cage which encapsulates both anions and cations in its central cavity.

Results and discussion

Synthesis and characterisation of $[Ru(L^{th})_3](PF_6)_2$

We have previously reported a series of molecular squares and coordination polymers with the thiophene-containing ligand L^{th}, in which the sulfur atom plays no part in the coordination chemistry but the thienyl unit just acts as a central spacer.[10] For example in $[M_4(L^{th})_6]X_8$ (M = Co, Ni, Cu) there is a square array of M(II) ions, with the four edges of the square bridged alternately by one or two ligands L^{th} (Fig. 2a). In these $[M_4(L^{th})_6]X_8$ assemblies *all* metal centres have the *mer* tris-chelate coordination geometry, as this is what the self-assembly process using labile M(II) ions selects.

Therefore, the question is: if an inert, pre-formed Ru(II) complex containing a mixture of *fac* and *mer* isomers is used in the assembly, would it afford a different product due to the constraint that some *fac* complex units must be present; or will the *mer* Ru(II) units be selected, and the *fac* units simply be ignored and excluded from the self-assembly process?

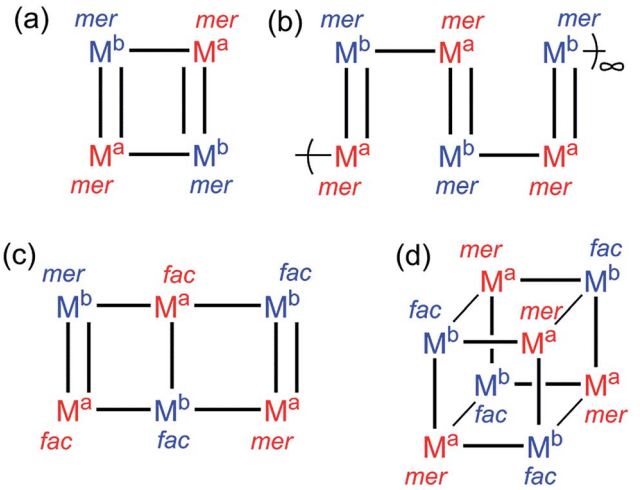

Fig. 2 Summary of the types of assembly discussed in this paper: black lines denote bridging ligands; the chemically different types of metal ion (M^a and M^b) are colour coded; and the *fac* or *mer* geometry at each position is indicated.

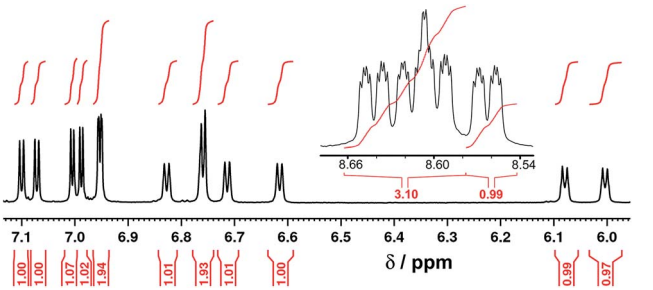

Fig. 4 Expansions of the ^{1}H NMR spectrum (400 MHz, CD_3CN) of $[Ru(L^{th})_3](PF_6)_2$ in Fig. 3. The 3 : 1 *mer*/*fac* mixture of isomers is clear from the presence of four different environments for each proton type with equal intensity, *e.g.* the expansion of the region around 8.6 ppm for coordinated pyridyl H^6 protons showing the presence of four doublets (with additional fine structure).

The mononuclear complex ligand $[Ru(L^{th})_3](PF_6)_2$ was prepared by reaction of >3 equivalents of L^{th} with one equivalent of $Ru(dmso)_4Cl_2$ in ethylene glycol at reflux, followed by anion metathesis and chromatographic purification during which the product was isolated as a single fraction with no apparent separation of *fac* and *mer* isomers. The ES mass spectrum confirmed the formation of the desired complex. The ^{1}H NMR spectrum of $[Ru(L^{th})_3](PF_6)_2$ showed that the expected[11] 1 : 3 *fac* : *mer* ratio of geometric isomers has formed. In the threefold-symmetric *fac* isomer all three ligands are equivalent, but this product is only one third as abundant as the *mer* isomer in which all three ligands are inequivalent. The result is the presence of four ligand environments with equal abundance, which the ^{1}H NMR spectrum shows clearly (Fig. 3 and 4).

Mixed metal structures incorporating $[Ru(L^{th})_3](PF_6)_2$ units

This mixture of geometric isomers for $[Ru(L^{th})_3](PF_6)_2$ does not provide exactly what is required for assembly of the complete squares (Fig. 2a) and chains (Fig. 2b) obtained using labile first-row metal ions, in which only the *mer* isomer is used.[9] Reaction of $[Ru(L^{th})_3](PF_6)_2$ (3 : 1 mixture of *mer* : *fac* isomers) with excess $Co(BF_4)_2$ (4.7 eq.) in methanol/dichloromethane solution instantly precipitated a yellow powder which was collected and thoroughly washed with methanol and dichloromethane, before recrystallisation from acetonitrile/ether to yield a crystalline product as fine yellow needles. Whereas the ES mass spectrum of the crude reaction mixture indicated the presence of RuL_3, $RuCoL_3$ and $Ru_2Co_2L_6$ species in solution, the X-ray crystal structure identified the structure of the product as the molecular square $[Ru_2Co_2(L^{th})_6](BF_4)_5(PF_6)_3 \cdot 2.5MeCN \cdot H_2O$ (Fig. 5 and 6) which has been able to select the best combination of anions from the mixture present to facilitate crystallisation.

The structure is essentially the same as those of the homonuclear squares reported previously.[10] It consists of two homochiral $M_2(L^{th})_2$ double helical units which are crosslinked by additional ligands to give the approximately square structure (with an alternating sequence of two and one bridging ligands spanning the edges, Fig. 2a). M···M separations are in the range 8.9–11.1 Å and M–M–M angles at the corners of the 'square' lie in the range 89.1–90.9°. All four metal centres have a *mer* tris-chelate coordination geometry. Due to the stepwise nature of the synthesis, in which every pendant pyrazolyl-pyridine binding site from the $[Ru(L^{th})_3]^{2+}$ units must bind to a Co(II) ion, we must have an alternating sequence of Ru(II) and Co(II) ions around the periphery of the square. This could adopt two possible orientations in the crystal: if the metal sites are labelled sequentially 1-2-3-4 around the ring we could have Ru(1)/Co(2)/Ru(3)/Co(4) or Co(1)/Ru(2)/Co(3)/Ru(4), with the difference in the scattering power of Ru and Co atoms making them easily distinguishable by X-ray crystallography. However it appears that the structure is crystallographically disordered

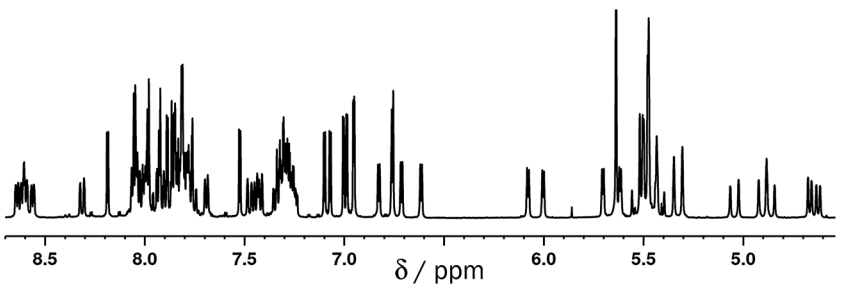

Fig. 3 ^{1}H NMR spectrum (400 MHz, CD_3CN) of $[Ru(L^{th})_3](PF_6)_2$.

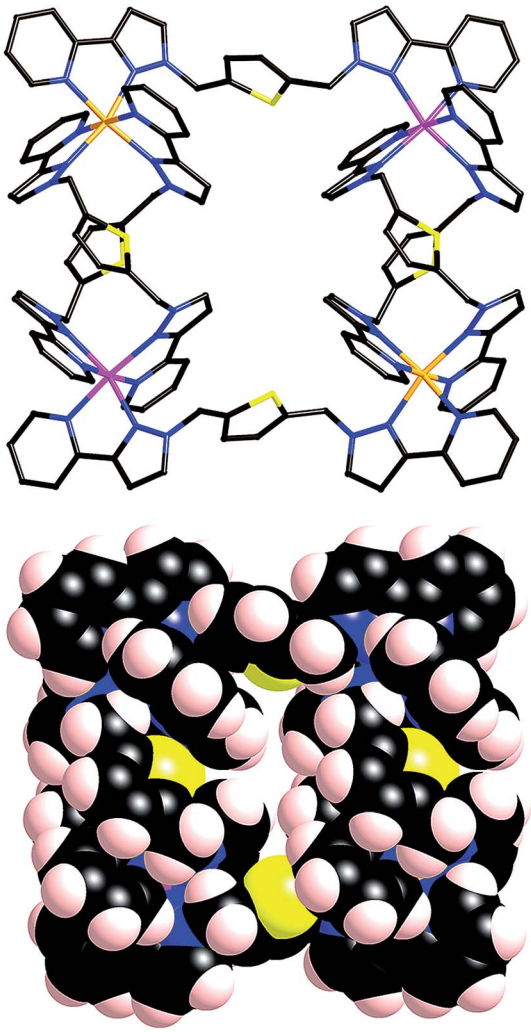

Fig. 5 Two views of the complete complex cation from the X-ray crystal structure of $[Ru_2Co_2(L^{th})_6](BF_4)_5(PF_6)_3$. Metal atom positions have been coloured differently to emphasise the alternating arrangement within each complex molecule, but disorder means that each metal atom site refines best as a 50 : 50 mixture of Ru and Co.

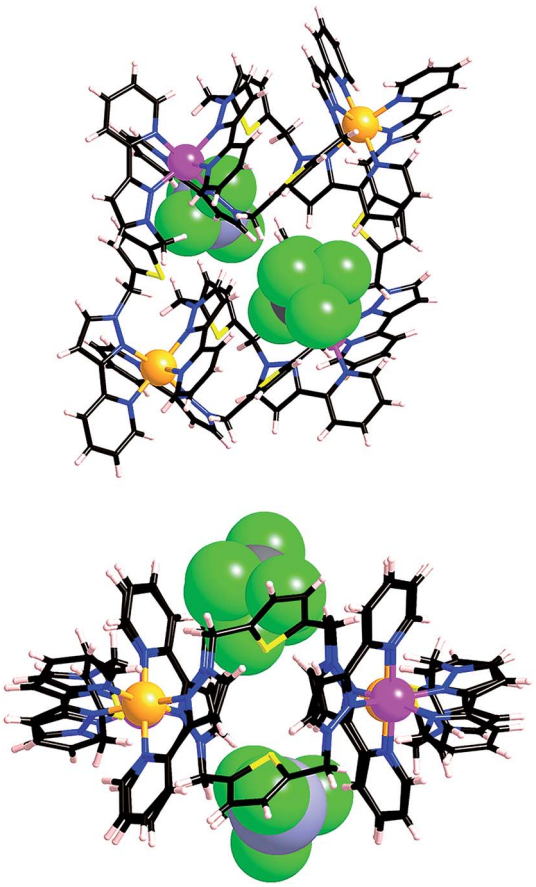

Fig. 6 Two views emphasising the interaction of one BF_4^- and one PF_6^- anions with the complex cation in the X-ray crystal structure of $[Ru_2Co_2(L^{th})_6](BF_4)_5(PF_6)_3$.

with the arrangements superimposed such that every metal atom site is best refined as 50% Ru and 50% Co. This is presumably facilitated by the similar coordination environments around the Ru(II) and Co(II) ions such that the ligand atoms appear in the same position if the metal ions are swapped over: thus only the metals are disordered, the ligand atom positions are not significantly affected by swapping the metal atom positions. This has been observed in other Ru(II)/Co(II) systems we have reported previously.[6b]

Two anions (PF_6^- and BF_4^-) sits on either side of the central region of the square, where there is a 'nest' of inwardly directed protons, forming numerous C–H···F hydrogen-bonding interactions (Fig. 6). The sulphur atoms of the thiophene rings apparently do not form any intermolecular interactions; there are instead, as with the homonuclear squares, intramolecular interactions between the exocyclic lone pairs and (electron-deficient) coordinated pyrazolyl rings on adjacent ligands in the helical M_2L_2 units.

The ^{1}H NMR spectrum of the redissolved crystals indicates that the structure observed in the solid state is preserved in solution (Fig. 7 and 8). Due to the paramagnetism of the high-spin Co(II) centres, the signals are shifted over the range of +100 to −80 ppm, as we have seen numerous times with structures of this type.[9] In homonuclear $[Co_4(L^{th})_6](BF_4)_4$, 27 ^{1}H NMR signals were observed in the NMR spectra, indicating 1.5 inequivalent ligand environments in agreement with the crystallographic symmetry.[10] However, with alternating Ru(II) and Co(II) centres in the mixed-metal complex Ru_2Co_2 complex we have lost a twofold symmetry element, resulting in three inequivalent ligand environments, each with no internal symmetry, and therefore we expect 54 independent proton resonances. Of these we expect those close to Co(II) to be most affected by the paramagnetism (broadened and/or shifted), and the protons close to the Ru(II) centres to be less affected.

This is apparent in the expansions in Fig. 8 in which we can see exactly the expected number of signals, split into two groups. Half of the signals occur in the 0–12 ppm region, from protons which are close to the Ru(II) but remote from Co(II); in some cases the fine coupling that is normal in spectra of diamagnetic compounds but usually lost for paramagnetic compounds is retained. The other half of the signals are far more widely dispersed (>15 and <−20 ppm) and arise from the protons closer

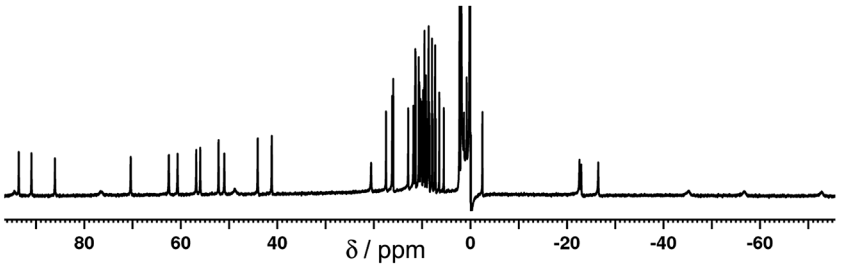

Fig. 7 ^{1}H NMR spectrum (400 MHz, CD_3CN) of $[Ru_2Co_2(L^{th})_6](BF_4)_4(PF_6)_4$.

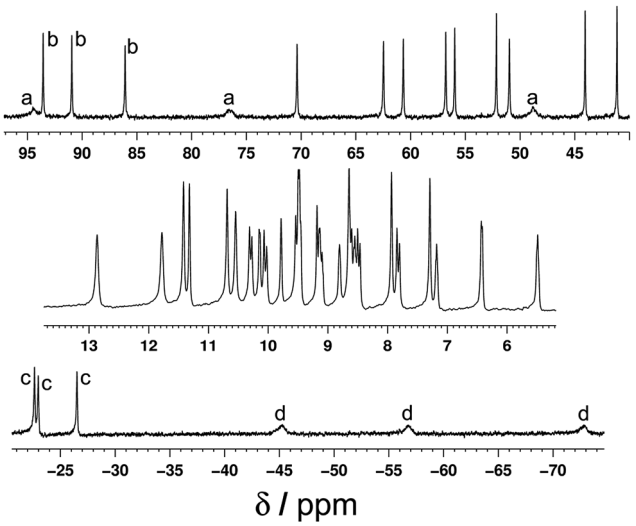

Fig. 8 Expansions of the ^{1}H NMR spectrum (400 MHz, CD_3CN) of $[Ru_2Co_2(L^{th})_6](BF_4)_4(PF_6)_4$ (most but not all regions of the spectrum in Fig. 7 are included). The labels a–d denote sets of three ligands corresponding to a particular ligand proton in each of three different environments.

to Co(II). In addition we can see in several places that the signals clearly come in sets of three, corresponding to the three ligand environments (*e.g.* the three broad signals between −40 and −80 ppm, and the three sharp signals between −20 and −30 ppm). Some of these are labelled in Fig. 8. Overall this spectrum clearly confirms that the structure observed in the solid state is retained in solution.

The DOSY spectrum in the 0–12 ppm region was measured, giving a single diffusion constant for all observed protons [log D (m^2 s^{-1}) = −9.2] that is characteristic of a large polynuclear assembly[9] and clearly not characteristic of a mononuclear complex.[6c] The mass spectrum of redissolved crystals showed that some fragmentation occurred under the mass spectral conditions; a series of peaks corresponding to $\{RuCo(L^{th})_3\}^{n+}$ species was observed, but importantly a series of peaks for the intact cation $\{Ru_2Co_2(L^{th})_6X_{8-n}\}^{n+}$ (with loss of varying numbers of anions) was also present.

Reaction of $[Ru(L^{th})_3](PF_6)_2$ (3 : 1 mixture of *mer* : *fac* isomers) with excess $Cd(ClO_4)_2$ (5.7 eq.) in methanol/dichloromethane solution instantly precipitated a yellow powder which was collected and thoroughly washed with methanol and dichloromethane, before recrystallisation from acetonitrile/ether to yield the product as fine yellow needles which gave analytical data consistent with the formulation $[CdRu(L^{th})_3](ClO_4)_2(PF_6)_2$. The ES mass spectrum is consistent with this, showing main signals corresponding to the $[CdRu(L^{th})_3]^{4+}$ cation associated with varying numbers of anions; the isotope pattern further confirms the formulation.

We expect this species this to have a similar structure to the homometallic Cd(II) complex $\{[Cd_2(L^{th})_3]X_4\}_\infty$, which is a one-dimensional coordination polymer consisting of an infinite chain of Cd(II) ions with an alternating arrangement of two and one bridging ligand between each adjacent pair of Cd(II) ions, as sketched in Fig. 2b: effectively, a linear chain of double helical $\{Cd_2(L^{th})_2\}^{4+}$ units connected end-to-end by additional L^{th} units which complete the sixfold coordination around each Cd(II) ion.[10] The *mer* tris-chelate geometry around every Cd(II) ion means that all three ligands are inequivalent. Consistent with this, the ^{1}H NMR spectrum of redissolved crystals of $[CdRu(L^{th})_3](ClO_4)_2(PF_6)_2$ revealed the presence of three independent ligand environments, each with no internal symmetry (Fig. 9) due to the inequivalence of Ru(II) and Cd(II) at either end of each ligand. For example it is apparent from the COSY spectrum that there are three pairs of doublets from the thienyl rings and six pairs of doublets from diastereotopic CH_2 groups (Fig. 9). Unfortunately, the crystals were extremely thin and weakly diffracting and the resultant structure is not of publishable quality, but it was sufficient to confirm that our assumption about the structure is correct: it is indeed a one-dimensional coordination polymer $\{[CdRu(L^{th})_3](ClO_4)_2(PF_6)_2\}_\infty$, similar to the homometallic Cd(II) analogue[10] but with (necessarily) an alternation of Ru(II) and Cd(II) ions along the chain.

Overall, even though a 3 : 1 *mer* : *fac* mixture of isomers of the relevant $[Ru(L^{th})_3]^{2+}$ building block was used, in both new examples shown here only the *mer* isomer was selected for incorporation into the mixed-metal assemblies – the *fac* $[RuL_3]^{2+}$ units are not used.

Synthesis and characterisation of $[Ru(L^{ph})_3](PF_6)_2$

The ligand L^{ph} has also been studied before: reaction of L^{ph} with transition metal dications in a 3 : 2 ratio leads to formation of approximately cubic $[M_8(L^{ph})_{12}]X_{16}$ cages which have the same type of S_6-symmetric metal framework as seen in the cages $[M_8(L^{naph})_{12}]X_{16}$: *viz.* two metal ions at either end of a long diagonal of the cube have a *fac* tris-chelate coordination environment whereas the other six have a *mer* geometry (*i.e.* a 3 : 1 *mer*/*fac*

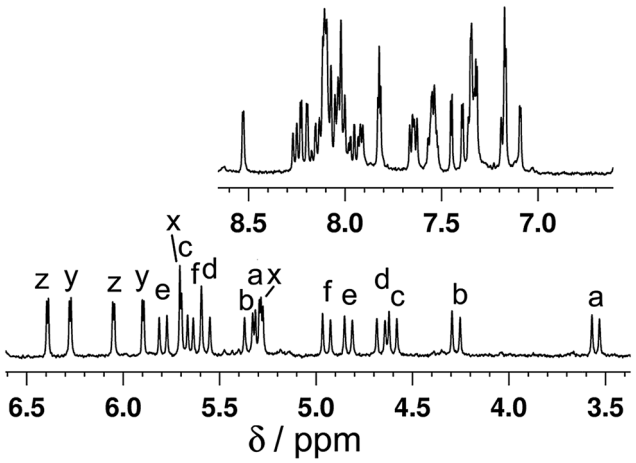

Fig. 9 ^{1}H NMR spectrum (400 MHz, CD_3CN) of $\{[CdRu(L^{th})_3](ClO_4)_2(PF_6)_2\}_\infty$. The six pairs of doublets from diastereotopic CH_2 groups are labelled a–f; the three pairs of doublets from the thienyl rings (with much smaller coupling constants) are labelled x, y and z. These assignments were made from a COSY spectrum and confirm that the complex in solution has three independent ligand environments, each with no internal symmetry, as required for the structural type in Fig. 2b.

ratio), with an inversion centre meaning that the cage as a whole is achiral.[9] In some cases we also observed formation of lower-symmetry $[M_6(L^{ph})_9]X_{12}$ assemblies which have a core structure reminiscent of a slightly bent 'open book' with metal ions at the four vertices and either end of the central spine, with bridging ligands arrayed along the edges [Fig. 2, structure (c)]. In these cases four of the six metal vertices (the central two and two at diagonally opposed corners) have a *fac* tris-chelate structure, with the other two metal vertices (the remaining two corners) having a *mer* tris-chelate geometry, giving a *mer* : *fac* ratio of 1 : 2. We might expect, therefore, that $[Ru(L^{ph})_3]^{2+}$ units could be incorporated into either or both of these types of assembly: either M_8L_{12} (Fig. 1) or M_6L_9 (Fig. 2c) depending on the relative amounts of *mer* and *fac* $[Ru(L^{ph})_3]^{2+}$ units that are available from its synthesis.

$[Ru(L^{ph})_3](PF_6)_2$ was prepared by reaction of $RuCl_2(dmso)_4$ with >3 equiv. L^{ph} in refluxing ethylene glycol, and after work-up a yellow solid was isolated whose analytical and ES mass spectrometric data were consistent with the formulation $[Ru(L^{ph})_3](PF_6)_2$. Interestingly, ^{1}H NMR spectroscopic analysis showed that the mixture was not formed as the expected statistical 3 : 1 *mer*/*fac* mixture: instead, the mixture contained an approximately 4 : 1 *mer*/*fac* ratio (Fig. 10 and 11). In areas where the separate peaks are clearly resolved we can identify three closely-spaced signals with an arbitrary intensity of 1.0 (corresponding to the three different ligand environments of the *mer* isomer), and a fourth signal (from the *fac* isomer) which has a relative intensity of approximately 0.72. This gives a *mer*/*fac* ratio of approximately 4.2 : 1. In this case we suggest that steric interactions between the three ligands, which will be more severe in the *fac* isomer, are sufficiently significant to give an excess of the kinetically favoured *mer* isomer compared to what is statistically expected (Fig. 11).[11]

This 4 : 1 *mer* : *fac* ratio of vertices has not been observed in any of the structures we have reported to date. We were therefore interested to see what types of heteronuclear assembly could be prepared using our as-isolated $[Ru(L^{ph})_3](PF_6)_2$ sample. Accordingly, $[Ru(L^{ph})_3](PF_6)_2$ (*ca.* 4 : 1 mixture of *mer* : *fac* isomers) was combined with $Co(BF_4)_2$ in dichloromethane/methanol solution. After filtration and washing, the resultant precipitate was recrystallized from acetonitrile, with slow diffusion of diisopropyl ether vapour into the solution yielding yellow X-ray quality crystals. The structural determination revealed the structure to be a $[Ru_3Co_3(L^{ph})_9](BF_4)_{12}$ 'open book' assembly (Fig. 12), which is structurally analogous to the homonuclear $[M_6(L^{ph})_9]^{12+}$ assemblies that we have seen before.[12]

The six metal ions are arranged in the manner of two squares sharing one edge, drawing comparison to an 'open book' structure. Both pairs of metal atoms forming outer edges of the 'book' are connected by two ligands in a double helical strand; four more ligands connect the outer metals to the 'spine' of the book, with the final ligand forming the 'spine' itself. Ru(II) and Co(II) ions necessarily occupy alternating sites within the framework, which again leads to two possible orientations of the heterometallic structure in the crystal. Again these are disordered such that unambiguous crystallographic labelling of each metal-ion site is not possible, but each site is refined as 50 : 50 Ru : Co. This is reflected in a moderate shortening of the metal–nitrogen bond lengths compared to what we observed in $[Co_6(L^{ph})_9](BF_4)_{12}$: an average M–N bond length of 2.09 Å is observed (ranging between 2.05–2.13 Å), compared to 2.12 Å in $[Co_6(L^{ph})_9](BF_4)_{12}$. The M···M separations around the edge of the 'book' are in the range 9.58–9.73 Å, and along the 'spine' the

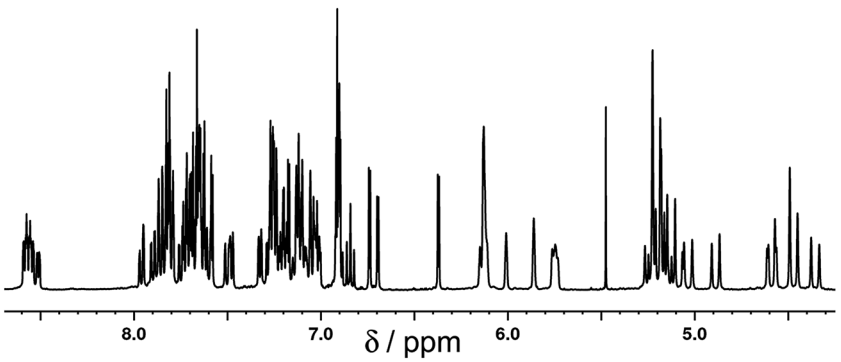

Fig. 10 ^{1}H NMR (CD_3CN, 400 MHz) spectrum of $[Ru(L^{ph})_3](PF_6)_2$ as a 4 : 1 mixture of *mer* : *fac* isomers (the peak at 5.5 ppm is a trace of CH_2Cl_2).

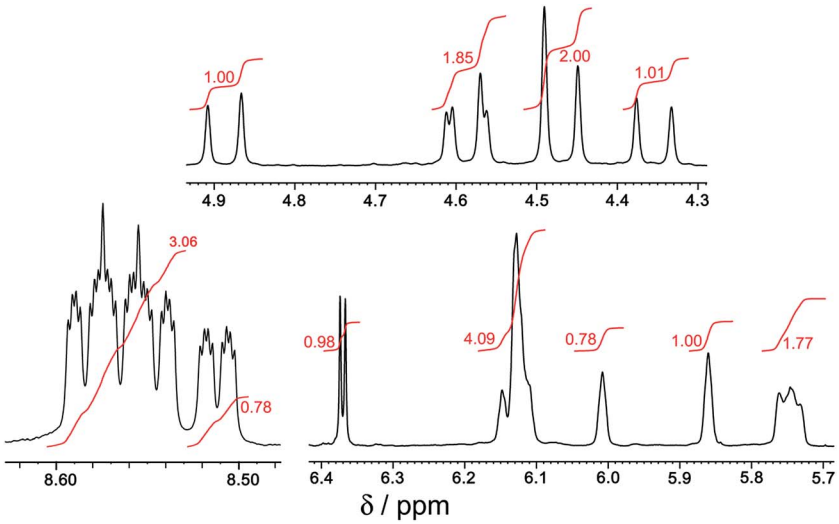

Fig. 11 Expansion of parts of Fig. 10; numbers in red are integral values.

separation is 10.50 Å. The angle between the two 'pages' of the book (*i.e.* between the two M_4 squares) is *ca.* 125°, resulting in two bowl-like cavities in which sit BF_4^- anions stabilised by numerous CH···F interactions (Fig. 12 and 13).

^{1}H NMR spectroscopy was of limited use due to the low symmetry. Homonuclear complexes $[M_6(L^{ph})_9]X_{12}$ possess only a C_2 axis in solution such that there are 4.5 independent ligand environments leading to 89 signals of relative intensity 2H and two (on the C_2 axis) of intensity 1H.[12b] In the mixed-metal complex this twofold symmetry is lost, such that we expect 180 independent ^{1}H signals, affording a highly complex NMR spectrum that cannot be meaningfully interpreted. However, ES mass spectrometry again confirmed the structural integrity of the complex in solution with signals corresponding to $\{[Ru_3Co_3(L^{ph})_9](BF_4)_{12-n}\}^{n+}$, *i.e.* the complete complex cation associated with varying numbers of anions, being observed with the correct *m*/*z* value and isotopic patterns.

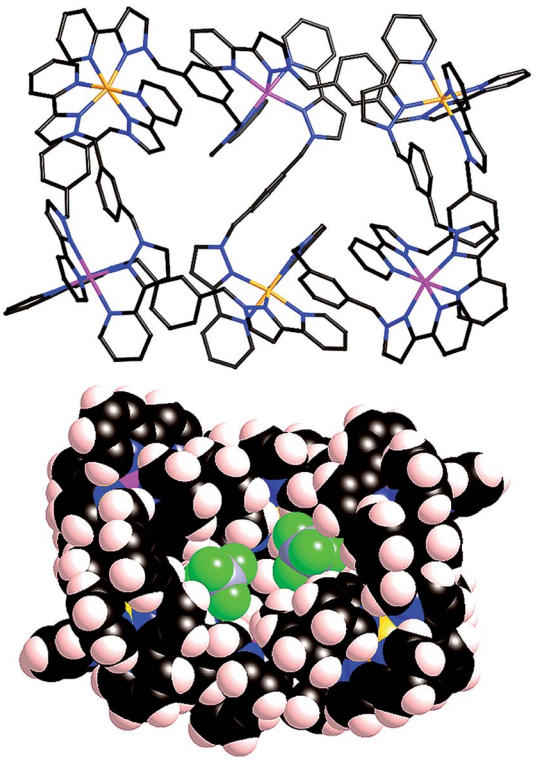

Fig. 12 Two views of the structure of $[Ru_3Co_3(L^{ph})_9](BF_4)_{12}$. Left: a view of the complete complex cation (all metal sites are 50 : 50 disordered, but in each molecule the metal ions necessarily alternate as indicated by the pink/orange colours). Right: a space-filling view emphasising the interaction of two anions with the complex cation.

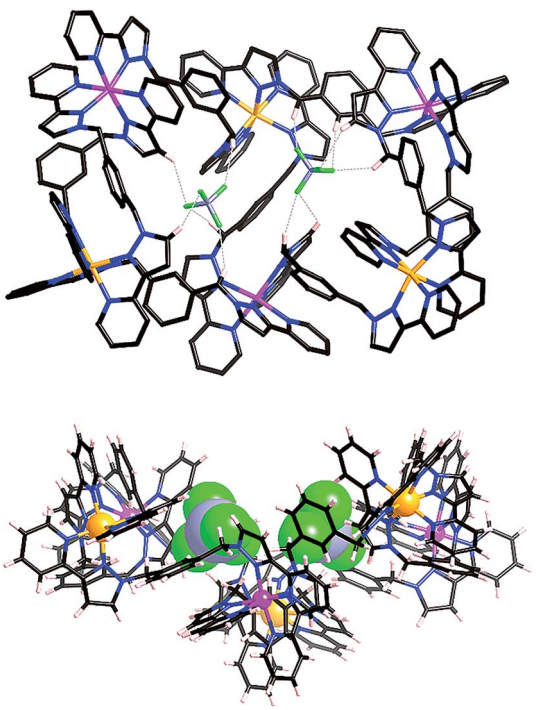

Fig. 13 Two additional views of the structure of $[Ru_3Co_3(L^{ph})_9](BF_4)_{12}$ emphasising the CH···F interactions between the two closely-associated BF_4^- anions and the complex cation.

In this structure four of the six metal sites have a *fac* tris-chelate geometry, *i.e.* of the three $[Ru(L^{ph})_3]^{2+}$ units that are incorporated, two are *fac* and one is *mer*, despite the excess of the *mer* isomer of $[Ru(L^{ph})_3]^{2+}$ in the sample used to generate the assembly. It follows that formation of $[Ru_3Co_3(L^{ph})_9](BF_4)_{12}$ does not make full use the available Ru(II) building blocks (as evidenced by the low isolated yield of the crystalline product): this contrasts with formation of the cubic cages $[Ru_4M_4(L^{naph})_{12}]X_{16}$ where the supply of *fac* and *mer* $[Ru(L^{naph})_3]^{2+}$ units is exactly in the 1 : 3 proportion required for the cage assembly to complete.[9] For this reaction of $[Ru(L^{ph})_3](PF_6)_2$ with Co(II) ions we assume that the remaining *mer* isomer of $[Ru(L^{ph})_3](PF_6)_2$ that is not required to assemble the 'book' structure forms some other heterometallic assembly with Co(II) ions but we were unable to establish its identity: ES mass spectra of the remaining solution after separation of crystalline $[Ru_3Co_3(L^{ph})_9](BF_4)_{12}$ showed only mononuclear complex species with no clear evidence for a larger assembly.

We were interested to see if we could isolate different assemblies containing $[Ru(L^{ph})_3]^{2+}$ units by changing the *mer* : *fac* ratio. Fletcher and co-workers demonstrated that the *mer* : *fac* ratio of a $[RuL_3]^{2+}$ complex based on a non-symmetrical chelating ligand can be skewed in favour of the *mer* isomer by performing the complexation under milder reaction conditions.[11] So we repeated the synthesis of $[Ru(L^{ph})_3](PF_6)_2$ at a much lower temperature, using refluxing ethanol/water mixture instead of refluxing ethylene glycol. After work-up a yellow solid was isolated which again analysed as $[Ru(L^{ph})_3](PF_6)_2$ but this time ^{1}H NMR analysis showed that it contained an approximately 7 : 1 *mer*/*fac* ratio of geometric isomers. Clearly, at lower temperature the reaction favours the kinetically more stable *mer* isomer. This does not make a huge difference to the isomeric composition which has changed from 80 : 20 *mer* : *fac* (preparation in ethylene glycol) to approximately 87 : 13 *mer* : *fac* (preparation in aqueous ethanol) but nonetheless this might affect the course of the assembly with Co(II) to give a heteronuclear species.

$[Ru(L^{ph})_3](PF_6)_2$ (7 : 1 mixture of *mer* : *fac* isomers) was reacted with one equivalent of $Co(BF_4)_2$ in dichloromethane/methanol at room temperature overnight. After workup, a yellow solid was collected which was slowly recrystallized from nitromethane by vapour diffusion with THF. This mixture was monitored by ES mass spectrometry over the course of two months whilst the recrystallization was occurring, revealing an interesting product evolution. Initially the spectrum was dominated by signals for a dinuclear species $\{[CoRu(L^{ph})_3]X_2\}^{2+}$ peaks [*m*/*z* 751, 785, 814; X = PF_6, BF_4 or F; Fig. 14a], but after a week, a series of peaks corresponding to the tetranuclear $\{[Co_2Ru_2(L^{ph})_6]X_5\}^{3+}$ appeared [*m*/*z* 1036, 1055, 1075, 1094 for the different anions; Fig. 14b] which we assume to be a square like that in Fig. 5. Finally, after several months, a series of peaks corresponding to octanuclear $\{[Co_4Ru_4(L^{ph})_{12}]X_{16-n}\}^{n+}$ had appeared [*m*/*z* 806, 942, 1123, 1377, 1757 for *n* = 8–4, respectively; Fig. 14c and 15]. Clearly assembly of the higher nuclearity species is slow under these conditions.

After several months, this solution yielded a crop of crystalline yellow blocks and orange shards. The yellow blocks were more abundant and of excellent X-ray quality. The structure revealed an octanuclear coordination cage cation, as expected on the basis of the mass spectrum, but with the formulation $[Ru_4Co_4(L^{ph})_{12}\{Na(BF_4)_4\}](PF_6)_6(BF_4)_7$ (Fig. 16–18), *i.e.* containing an additional sodium cation and an associated anion. The Ru_4Co_4 metal framework is approximately cubic, with alternating Ru(II) and Co(II) ions at each metal site, as expected. Ru⋯Co separations along the edges are in the range 9.79–10.63 Å; M–M–M angles are in the range 80.0–103.0°. However the framework type is unexpectedly different from any type of cubic coordination cage that we have seen before.

This octanuclear cage crystallised in the tetragonal space group $P\bar{4}2_1m$, with S_4 molecular symmetry (axis through the centre of the face of the cube), such that one quarter of the complex cation is crystallographically unique. The asymmetric unit contains one Co(II) ion with a *fac* tris-chelate geometry and one Ru(II) ion with a *mer* tris-chelate geometry. This has the consequence of the complete cube having alternating *fac* (Co) and *mer* (Ru) metal sites around the framework, an arrangement

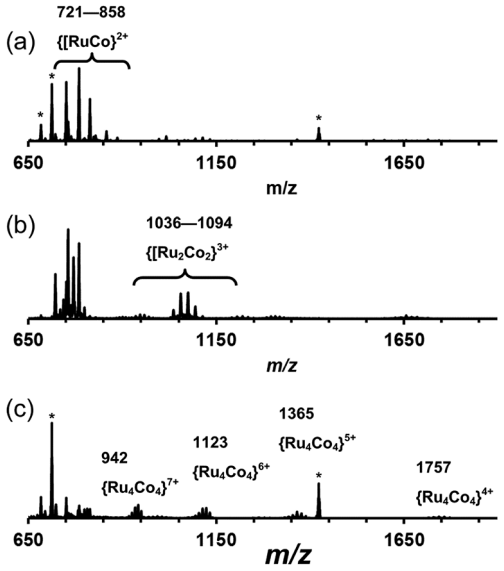

Fig. 14 Series of ES mass spectra following the evolution of the product mixture of $[Co_nRu_n(L^{ph})_{3n}]X_{4n}$. (a) Product mixture after 1 day; (b) product mixture after 1 week; (c) product mixture after 2 months. Peaks labelled * are due to $[Ru(L^{ph})_3]^{2+}$, arising from fragmentation of the larger complexes. The presence of several closely-spaced peaks for each type of assembly arises because of the presence of a mixture of anions in solution.

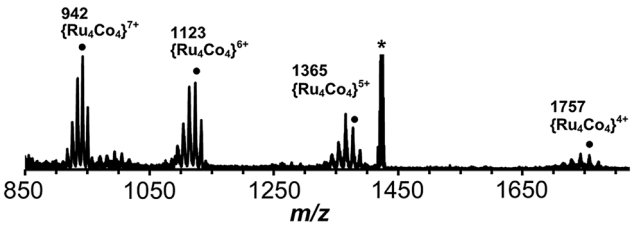

Fig. 15 Expansion of the ES mass spectrum of $[Co_4Ru_4(L^{ph})_{12}]X_{16}$ (see Fig. 14c). The *m*/*z* values given are for the peaks labelled ● for which $X_{16-n} = \{(PF_6)_{15}(BF_4)\} - nPF_6$.

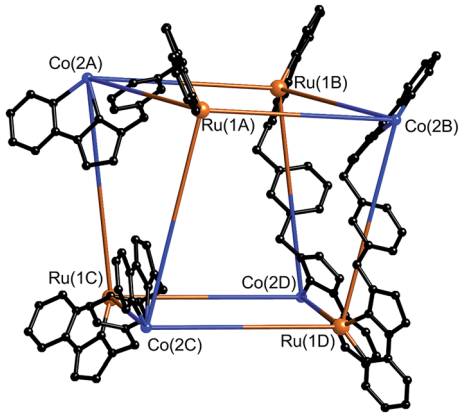

Fig. 16 Partial view of the complex cation of $[Ru_4Co_4(L^{ph})_{12}\{Na(BF_4)_4\}](PF_6)_6(BF_4)_7$. All Ru atoms and all Co atoms are crystallographically equivalent, but the two metal ion types are *not* disordered. Only four (crystallographically equivalent) ligands are shown.

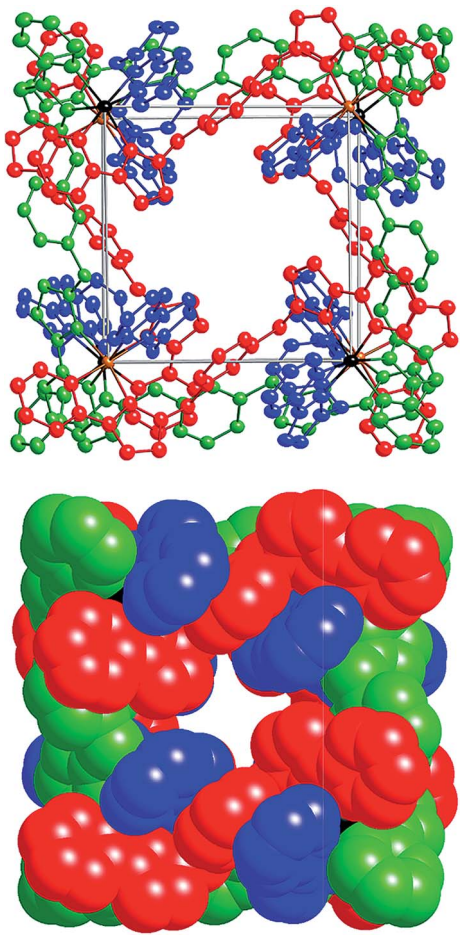

Fig. 17 Left: View of the complete complex cation of $[Ru_4Co_4(L^{ph})_{12}\{Na(BF_4)_4\}](PF_6)_6(BF_4)_7$. Thermal ellipsoids shown at 40% probability, and crystallographically equivalent ligands are coloured the same. Right: Space-filling view of the complex cation from the same perspective.

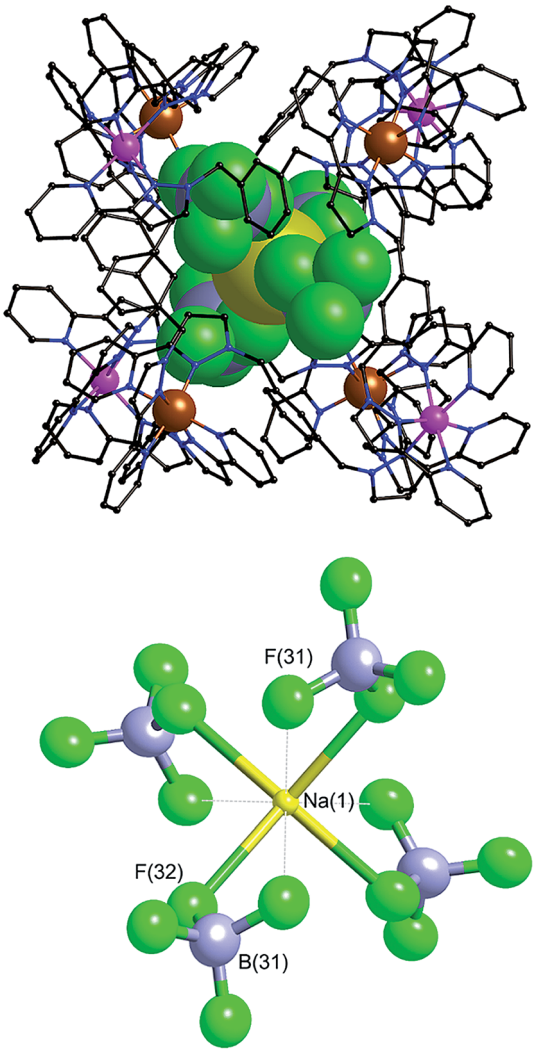

Fig. 18 Two views of the structure of the complex $[Ru_4Co_4(L^{ph})_{12}\{Na(BF_4)_4\}](PF_6)_6(BF_4)_7$. Left: View of the complete octanuclear cage (wireframe view), with the bound $[Na(BF_4)_4]^{3-}$ shown in space-filling mode. Right: Thermal ellipsoid plot of the bound guest $[Na(BF_4)_4]^{3-}$, with ellipsoids shown at 40% probability.

which has not occurred in any previous cages of this family, even in the homonuclear analogues.[8–10] Identification of the metal at each site turned out to be trivial; significantly different M–N bond lengths [average 2.07 Å (*mer*) and 2.13 Å (*fac*)] and physically unreasonable thermal parameters upon mislabelling confirmed that the *mer* site is occupied exclusively by Ru atoms, and the *fac* site by Co atoms, so the different metal types are now crystallographically ordered because of their different coordination geometry. Extensive π-stacking between the electron-rich and electron-deficient parts of adjacent ligands is clear around the periphery of the complex.

This new S_4 structure for an M_8L_{12} cubic cage is interesting in itself, but equally interesting is what lies inside the cavity. Usually with this family of cages, a solvent molecule or anion is found lying close to the convergent set of methylene protons surrounding the *fac* vertices, which form weak H-bond donor sites that can interact with electronegative atoms.[9] As there are

four *fac* tris-chelate vertices in this structure, there are potentially four recognition sites at which electron-rich guests may form hydrogen bonds with the interior surface of the cage. In this crystal structure, all of these sites are occupied.

Within the cavity there lie four tetrafluoroborate anions, one directed towards each *fac* vertex [around a Co(II) ion]. The organisation of these four anions into a tetrahedral array – dictated by the positioning of the four *fac* tris-chelate sites in the cube – results in formation of a central space surrounded by these four tetrafluoroborate anions – a 'cavity within a cavity', within which is bound a sodium cation which arises adventitiously (Fig. 18 and 19) and is most likely leached from the glassware. Two pieces of evidence support the assignment of the central atom as Na. Firstly, the distance to the nearest F atoms of the surrounding tetrafluoroborate anions is consistent with an Na···F dative interaction [Na(1)–F(32), 2.46 Å; Na(1)–F(31), 2.82 Å].[13] Secondly, the thermal parameters become nonsensical when the atom is labelled differently (*e.g.* as K^+ or Co^{2+}). The arrangement of four anions in close proximity to one another inside the Ru_4Co_4 cage cavity is stabilised by coordination of all of them to Na^+, as well as by numerous CH···F contacts between the ligands in the cage superstructure ligand and the encapsulated anions, the shortest of which is 2.23 Å between H(25C) and F(32).

Formation of this 'complex within a complex' requires three layers in a hierarchical self-assembly: the self-assembled Ru_4Co_4 cage encapsulates a tetrahedral array of four tetrafluoroborate anions, which in turn surround a central Na^+ ion. This has parallels with the metallacrowns first reported by Pecoraro and co-workers,[14] in which a transition-metal/ligand cyclic array based on Mn(III) ions and salicyl-hydroximate ligands results in an O-donor cavity whose structure is reminiscent of a crown ether, which accordingly coordinates additional alkali metal cations in the centre. It is also related to the observation from both Lindoy and co-workers[15a] and Nitschke and co-workers[15b] of the binding of tetrahalometallate anions as guests in the cavities of cationic M_4L_6 tetrahedral cage complexes. Addition of extra sodium salts to the crystallisation did not significantly improve the yield of crystalline material.

That this product should form containing exclusively the *mer* isomer of $[Ru(L^{ph})_3](PF_6)_2$ can be rationalised on the basis that a large excess of this isomer was available for the cage-forming reaction. The minor product from the crystallisation (the orange shards) unfortunately did not yield any single crystals of sufficient quality to determine the crystal structure. The ES mass spectrum of these crystals revealed a mixture of tetranuclear $[Ru_2Co_2(L^{ph})_6]^{8+}$ and octanuclear $[Ru_4Co_4(L^{ph})_{12}]^{16+}$ species associated with varying numbers of anions. These may be presumed to incorporate the *fac*-$[Ru(L^{ph})_3](PF_6)_2$ units in some form of assembly with Co(II) ions but could not be characterised further; the ^{1}H NMR spectra were very complex and uninformative.

Finally we note that the difference in the nature of the products isolated by combination of $[Ru(L^{ph})_3](PF_6)_2$ (4 : 1 *mer* : *fac* ratio) with Co(II) [which afforded the Ru_3Co_3 'open book' as the only isolable crystalline product] and $[Ru(L^{ph})_3](PF_6)_2$ (7 : 1 *mer* : *fac* ratio) with Co(II) [which afforded the new Ru_4Co_4 cube] cannot just be ascribed to the slightly higher proportion of the *mer* isomer of $[Ru(L^{ph})_3](PF_6)_2$ in the latter case. The solvent systems used to grow the crystals were also different (MeCN/^{i}Pr$_2$O in the former case; $MeNO_2$/thf in the latter case) which could play an important role in determining which type of assembly is least soluble and therefore dominates the crystallisation.

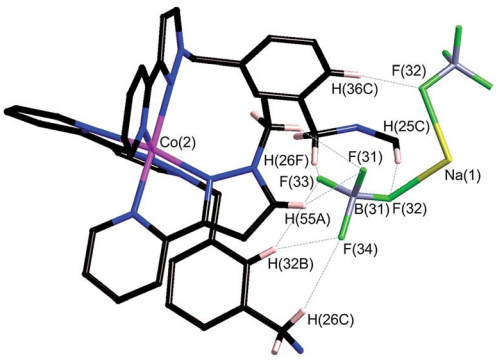

Fig. 19 Partial view of one of the *fac*-$[Co(L^{ph})_3]^{2+}$ vertices in the $[Ru_4Co_4(L^{ph})_{12}]^{16+}$ complex cation, with CH···F interactions between ligands and the encapsulated $(BF_4)^-$ anions indicated by dashed lines.

Conclusions

We have explored two families of heteronuclear complexes in which pre-formed, kinetically stable $[Ru(L^{th})_3]^{2+}$ and $[Ru(L^{ph})_3]^{2+}$ units (in the form of as-isolated mixtures of *fac* and *mer* isomers) are combined with labile M(II) ions (M = Co or Cd) to give Ru/M assemblies in which the Ru(II) and M(II) ions alternate in the metal array. With L^{th} as the bridging ligand we isolated the molecular square $[Ru_2Co_2(L^{th})_6](BF_4)_4(PF_6)_4$ and the one-dimensional coordination polymer $\{[CdRu(L^{th})_3](ClO_4)_2(PF_6)_2\}_\infty$. Both are based on heterodinuclear $\{RuM(L^{th})_2\}^{4+}$ double helicate units, with two connected side by side by additional bridging ligand to form a Ru_2Co_2 molecular square; or a one-dimensional sequence linked end-to-end to give an alternating $\{RuCd\}_\infty$ chain.

With L^{ph} as the bridging ligand we isolated two quite different assemblies with Co(II) which contain different proportions of *fac* and *mer* Ru(II) units. These are the rectangular 'open-book' array $[Ru_3Co_3(L^{ph})_9](BF_4)_{12}$ which contains a 2 : 1 proportion of *fac*/*mer* metal centres; and the cubic $[Ru_4Co_4(L^{ph})_{12}\{Na(BF_4)_4\}](PF_6)_6(BF_4)_7$ cage which is a new structural type containing all *mer* Ru(II) vertices and all *fac* Co(II) vertices. The cavity of the cubic cage contains a tetrahedral array of fluoroborate anions which in turn are connected to a central Na(I) ion – a metal complex as the guest inside a metal complex.

Experimental section

General details

Metal salts and all organic reagents were purchased from Alfa or Sigma-Aldrich and used as received. NMR spectra were recorded on Bruker DRX 500 MHz, Bruker AV-III 400 MHz or AV-I 250 MHz instruments. Electrospray mass spectra were recorded on a Micromass LCT instrument. UV/Vis absorption spectra were measured on a Varian Cary 50 spectrophotometer. The ligands L^{th}

and L^{ph} were prepared according to the published methods.[10,12] $Ru(dmso)_4Cl_2$ was prepared by the literature method.[16]

Syntheses of mononuclear Ru(II) complexes

(i) $[Ru(L^{th})_3](PF_6)_2$ (4 : 1 *mer* : *fac* ratio). A solution of L^{th} (0.14 g, 0.35 mmol) was stirred rapidly in refluxing ethylene glycol (50 cm^3) until dissolved. To this was added a solution of $RuCl_2(dmso)_4$ (0.02 g, 0.04 mmol) in H_2O/ethylene glycol (3 : 100, 103 cm^3) by dropping funnel over 3 hours, and then the orange mixture was stirred at reflux for 14 h. The solution was cooled to 25 °C and excess saturated $KPF_{6(aq.)}$ was added. The product was extracted with dichloromethane, dried over $MgSO_4$, and evaporated to dryness.

The product was purified by column chromatography on silica. Elution with MeCN–water–saturated aqueous KNO_3 (100 : 10 : 1, v/v) resulted in two yellow bands moving down the column – the second, major band was collected. After removing acetonitrile by rotary evaporation, excess saturated aqueous KPF_6 was added and the product was extracted from the resulting suspension into dichloromethane. The organic layer was separated, dried over $MgSO_4$, and the solvent removed *in vacuo* to yield $[Ru(L^{th})_3](PF_6)_2$, 3 : 1 *mer* : *fac* ratio, as a yellow solid. Yield: 0.04 g, 54%.

ESMS: *m*/*z* 648 $(M - 2PF_6)^{2+}$, 432 $(M - 2PF_6 + H)^{3+}$. UV/Vis in MeCN [λ_{max}/nm (10^{-3} ε/M^{-1} cm^{-1})]: 396 (13.1), 281 (72.8), 243 (81.5). Found: C, 48.2; H, 3.9; N, 15.1%. Required for $C_{66}H_{54}N_{18}P_2F_{12}RuS_3 \cdot 3H_2O$: C, 48.3; H, 3.7; N, 15.4%.

(ii) $[Ru(L^{th})_3](PF_6)_2$ (7 : 1 *mer* : *fac* ratio). A solution of L^{ph} (0.30 g, 0.76 mmol) in ethanol (100 cm^3) and H_2O (20 cm^3) was stirred under reflux until fully dissolved. To this was added a solution of $RuCl_2(dmso)_4$ (0.05 g, 0.11 mmol) in ethanol/H_2O (7 : 5 v/v, 60 cm^3) by dropping funnel over 3 hours, and then the yellow mixture was stirred at reflux in the dark for 14 h. After cooling the red mixture and diluting with H_2O, excess ligand was removed by washing with chloroform. Addition of saturated $KPF_{6(aq.)}$ afforded a yellow precipitate, which was purified by column chromatography on silica. Elution with MeCN–water–saturated aqueous KNO_3 (100 : 10 : 1 v/v) resulted in a broad yellow band moving down the column which was collected. After removing acetonitrile by rotary evaporation, excess saturated aqueous KPF_6 was added and the product was extracted from the suspension into dichloromethane. The organic layer was separated, dried over $MgSO_4$, and the solvent removed *in vacuo* to yield $[Ru(L^{ph})_3](PF_6)_2$ as a yellow solid (7 : 1 *mer* : *fac* ratio). Yield: 0.24 g, 78%. ESMS *m*/*z* 1423 $(M - PF_6)^+$, 639 $(M - 2PF_6)^{2+}$, 426 $(M + H - 2PF_6)^{3+}$. Found: C, 54.7; H, 4.1; N, 15.8%. Required for $C_{72}H_{60}N_{18}P_2F_{12}Ru$: C, 55.1; H, 3.9; N, 16.1%.

Synthesis of polynuclear heterometallic complexes

(i) $[Ru_2Co_2(L^{th})_6](BF_4)_4(PF_6)_4$. To a stirred solution of $[Ru(L^{th})_3](PF_6)_2$ (0.02 g, 0.013 mmol) in dichloromethane (5 cm^3) was added a solution of $Co(BF_4)_2 \cdot 6H_2O$ (0.02 g, 0.059 mmol) in methanol (5 cm^3). After stirring at RT overnight, the yellow precipitate was collected by filtration on a membrane filter and washed with dichloromethane and methanol. Slow diffusion of diethyl ether into a solution of the solid in acetonitrile gave the product as yellow needles in 65% yield. ESMS (selected peaks): *m*/*z* 1675, $\{[Ru_2Co_2(L^{th})_3](BF_4)_4(PF_6)_2\}^{2+}$; 1126, $\{[Ru_2Co_2(L^{th})_3](BF_4)(PF_6)_4\}^{3+}$; 1107, $\{[Ru_2Co_2(L^{th})_3](BF_4)_2(PF_6)_3\}^{3+}$; 1087, $\{[Ru_2Co_2(L^{th})_3](BF_4)_3(PF_6)_2\}^{3+}$; 1068, $\{[Ru_2Co_2(L^{th})_3](BF_4)_2(PF_6)_3\}^{3+}$; 1049, $\{[Ru_2Co_2(L^{th})_3](BF_4)_5\}^{3+}$; 731, $\{[RuCo(L^{th})_3](BF_4)F\}^{2+}$; 458, $\{[RuCo(L^{th})_3]F\}^{3+}$; 339, $\{[RuCo(L^{th})_3]\}^{4+}$. UV/Vis in MeCN [$\lambda_{max}$/nm ($10^{-3}$ ε/M^{-1} cm^{-1})]: 396 (25.5), 283 (142.0), 242 (157.7). Found: C, 41.6; H, 3.5; N, 12.9%. Required for $C_{132}H_{108}B_4Co_2F_{40}N_{36}P_4Ru_2S_6 \cdot 8H_2O$: C, 41.9; H, 3.3; N, 13.3%.

(ii) $[RuCd(L^{th})_3](ClO_4)_2(PF_6)_2$. To a stirred solution of $[Ru(L^{th})_3](PF_6)_2$ (0.02 g, 0.013 mmol) in dichloromethane (5 cm^3) was added a solution of $Cd(ClO_4)_2 \cdot 6H_2O$ (0.03 g, 0.072 mmol) in methanol (5 cm^3). After stirring overnight, the yellow precipitate was collected by filtration on a membrane filter and washed with dichloromethane and methanol. Slow diffusion of diethyl ether into a solution of the solid in acetonitrile gave the product as yellow needles in 59% yield. ESMS (selected peaks): *m*/*z* 1707, $\{[RuCd(L^{th})_3](ClO_4)_3\}^+$; 1106, $\{[Ru_2Cd_2(L^{th})_6](ClO_4)_5\}^{3+}$; 804, $\{[RuCd(L^{th})_3](ClO_4)_2\}^{2+}$; 503, $\{[RuCd(L^{th})_3](ClO_4)\}^{3+}$; 352, $\{[RuCd(L^{th})_3]\}^{4+}$. UV/Vis in MeCN [$\lambda_{max}$/nm ($10^{-3}$ ε/M^{-1} cm^{-1})]: 396 (13.2), 282 (72.0), 242 (81.3). Found: C, 42.3; H, 4.7; N, 12.0%. Required for $C_{66}H_{54}CdCl_2F_{12}N_{18}O_8P_2RuS_3 \cdot 6H_2O \cdot 3Et_2O \cdot MeCN$: C, 42.3; H, 4.4; N, 11.7%.

(iii) $[Ru_4Co_4(L^{ph})_{12}](BF_4)_8(PF_6)_8$. To a stirred solution of $[Ru(L^{ph})_3](PF_6)_2$ (7 : 1 mixture of *mer* : *fac* isomers; 0.073 g, 0.047 mmol) in dichloromethane (10 cm^3) was added a solution of $Co(BF_4)_2 \cdot 6H_2O$ (0.016 g, 0.047 mmol) in methanol (10 cm^3). After an overnight stir, the mixture was evaporated to dryness and then washed with dichloromethane and methanol. The mixture was then collected on a membrane filter and then extracted with nitromethane. Slow diffusion of tetrahydrofuran vapour into the nitromethane solution over two months gave the product as yellow blocks in 35% isolated yield, and orange shards in 14% isolated yield. ESMS (selected peaks): *m*/*z* 1757, $([Ru_4Co_4(L^{ph})_{12}](BF_4)(PF_6)_{11})^{4+}$; 1743, $([Ru_4Co_4(L^{ph})_{12}](BF_4)_2(PF_6)_{10})^{4+}$; 1377, $([Ru_4Co_4(L^{ph})_{12}](BF_4)(PF_6)_{10})^{5+}$; 1365, $([Ru_4Co_4(L^{ph})_{12}](BF_4)_2(PF_6)_9)^{5+}$; 1123, $([Ru_4Co_4(L^{ph})_{12}](BF_4)(PF_6)_9)^{6+}$; 1114, $([Ru_4Co_4(L^{ph})_{12}](BF_4)_2(PF_6)_8)^{6+}$; 942, $([Ru_4Co_4(L^{ph})_{12}](BF_4)(PF_6)_8)^{7+}$; 934, $([Ru_4Co_4(L^{ph})_{12}](BF_4)_2(PF_6)_7)^{7+}$; 806, $([Ru_4Co_4(L^{ph})_{12}](BF_4)(PF_6)_7)^{8+}$; 799, $([Ru_4Co_4(L^{ph})_{12}](BF_4)_2(PF_6)_6)^{8+}$. Elemental analytical data was consistent with the presence of water of crystallisation due to the desolvated material being hygroscopic. Found: C, 46.2; H, 3.6; N, 13.0%. Required for $C_{288}H_{240}B_9NaCo_4F_{84}N_{72}P_8Ru_4 \cdot 12H_2O$: C, 45.9; H, 3.5; N, 13.4%.

(iv) $[Ru_3Co_3(L^{ph})_9](BF_4)_{12}$. To a stirred solution of $[Ru(L^{ph})_3](PF_6)_2$ (4 : 1 mixture of *mer* : *fac* isomers; 0.053 g, 0.034 mmol) in dichloromethane (10 cm^3) was added a solution of $Co(BF_4)_2 \cdot 6H_2O$ (0.126 g, 0.370 mmol) in methanol (10 cm^3). After an overnight stir, the mixture was evaporated to dryness and then washed with dichloromethane and methanol on a membrane filter. Slow diffusion of diisopropyl ether into a solution of the solid in nitromethane gave the product as yellow laths in low yield (17%). ESMS (selected peaks): *m*/*z* 2440, $([Ru_3Co_3(L^{ph})_9](BF_4)_{10})^{2+}$; 1599, $([RuCo(L^{ph})_3](BF_4)_3)^+$; 1177, $([Ru_3Co_3(L^{ph})_9](BF_4)_8)^{4+}$; 1036, $([Ru_2Co_2(L^{ph})_6](BF_4)_5)^{3+}$; 924, $([Ru_3Co_3(L^{ph})_9](BF_4)_7)^{5+}$; 756, $([RuCo(L^{ph})_3](BF_4)_2)^{2+}$; 452, $([RuCo(L^{ph})_3]F)^{3+}$. UV/Vis in MeCN [λ_{max}/nm (10^{-3} ε/M^{-1} cm^{-1})]: 396 (38.7), 282 (216.1), 244 (206.7).

Table 1 Crystal parameters, data collection and refinement details for the structures in this paper[a]

Complex	$2\{[Ru_2Co_2(L^{th})_6]\}(BF_4)_{10}(PF_6)_6\cdot 5MeCN\cdot 2H_2O$	$[Ru_4Co_4(L^{ph})_{12}]Na(BF_4)_{11}(PF_6)_6\cdot 8MeNO_2$	$2\{[Ru_3Co_3(L^{ph})_9](BF_4)_{12}\}\cdot 11MeNO_2\cdot 3H_2O$
Formula	$C_{274}H_{235}B_{10}Co_4F_{76}N_{77}P_6Ru_4S_{12}$	$C_{296}H_{264}B_{11}Co_4F_{80}N_{80}NaO_{16}P_6Ru_4$	$C_{443}H_{399}B_{24}Co_6F_{96}N_{119}O_{25}Ru_6$
Molecular weight	7401.02	7685.58	10 833.23
T, K	100(2)	100(2)	100(2)
Crystal system	Monoclinic	Tetragonal	Triclinic
Space group	$P2_1/c$	$P\bar{4}2_1m$	$P\bar{1}$
a, Å	17.3091(12)	31.3553(12)	26.036(5)
b, Å	42.874(3)	31.3553(12)	27.068(6)
c, Å	22.2336(16)	21.7210(8)	42.869(10)
α, °	90	90	84.340(5)
β, °	103.1010(18)	90	88.764(5)
γ, °	90	90	87.336(8)
V, Å^3	16 070(2)	21 355.1(18)	30 027(11)
Z	2	2	2
ρ, g cm^{-3}	1.529	1.195	1.198
Crystal size, mm^3	0.07 × 0.03 × 0.01	0.2 × 0.2 × 0.2	0.32 × 0.16 × 0.08
μ, mm^{-1}	0.556	0.403	0.396
Independent data, restraints, parameters	17 217/139/1901	15 202/832/840	62 175/302/1895
Final R_1, wR_2[b]	0.1088, 0.2800	0.0794, 0.2209	0.1289, 0.3298

[a] The compositions are necessarily approximate as they do not include solvent molecules eliminated from the refinement as part of the 'SQUEEZE' process. [b] The value of R_1 is based on 'observed' data with $I > 2\sigma(I)$; the value of wR_2 is based on all data.

X-ray crystallography

Diffraction data for the structures $[Ru_4Co_4(L^{ph})_{12}]Na(BF_4)_{11}(PF_6)_6\cdot 8MeNO_2$ and $2\{[Ru_3Co_3(L^{ph})_9](BF_4)_{12}\}\cdot 11MeNO_2\cdot 3H_2O$ were collected on a Bruker Apex-II diffractometer at the University of Sheffield. Diffraction data for $2\{[Ru_2Co_2(L^{th})_6]\}(BF_4)_{10}(PF_6)_6\cdot 5MeCN\cdot 2H_2O$ were collected by the National Crystallographic Service using a synchrotron radiation source.[17] In each case a crystal was removed from the mother liquor, coated with oil, and transferred rapidly to a stream of cold N_2 on the diffractometer to prevent rapid decomposition due to solvent loss which occurred in all cases. In all cases, after integration of the raw data, and before merging, an empirical absorption correction was applied (SADABS)[18] based on comparison of multiple symmetry-equivalent measurements. The structures were solved by direct methods and refined by full-matrix least squares on weighted F^2 values for all reflections using the SHELX suite of programs.[19] Pertinent crystallographic data are collected in Table 1.

In all cases crystals exhibited the usual problems of this type of structure, *viz.* weak scattering due to a combination of poor crystallinity, solvation, and disorder of anions/solvent molecules. In each case the basic structure and connectivity of the complex cation could be unambiguously determined with reasonable precision. Extensive use of geometric restraints on aromatic rings and anions, and restraints on aromatic displacement parameters, were required to keep refinements stable. Solvent molecules and anions that could be modelled satisfactorily were included in the final refinements; in all cases large regions of diffuse electron density that could not be modelled (from disordered solvents/counter ions) were removed from the refinement, using the SQUEEZE function in PLATON.[20] Full details of these issues and how they were handled are given in the individual CIFs; it should be noted that the compositions/formulae of the crystals as given in Table 1 are necessarily an approximation. CCDC deposition numbers: 1433701–1433703.†

Acknowledgements

We thank the EPSRC for financial support (grant EP/K003224/1), and Dr Andrew Stephenson for synthesis of a sample of L^{th}.

References

1 (*a*) D. Fiedler, D. H. Leung, R. G. Bergman and K. N. Raymond, *Acc. Chem. Res.*, 2005, **38**, 349; (*b*) M. Fujita, M. Tominaga, A. Hori and B. Therrien, *Acc. Chem. Res.*, 2005, **38**, 369; (*c*) M. D. Ward, *Chem. Commun.*, 2009, 4487; (*d*) J. J. Perry, J. A. Perman and M. J. Zaworotko, *Chem. Soc. Rev.*, 2009, **38**, 1400; (*e*) H. Amouri, C. Desmarets and J. Moussa, *Chem. Rev.*, 2012, **112**, 2015; (*f*) A. F. Williams, *Coord. Chem. Rev.*, 2011, **255**, 2104; (*g*) Z. Laughrey and B. Gibb, *Chem. Soc. Rev.*, 2011, **40**, 363; (*h*) P. Jin, S. J. Dalgarno and J. L. Atwood, *Coord. Chem. Rev.*, 2012, **254**, 1760; (*i*) R. J. Chakrabarty, P. S. Mukherjee and P. J. Stang, *Chem. Rev.*, 2011, **111**, 6810; (*j*) Y. Inokuma, M. Kawano and M. Fujita, *Nat. Chem.*, 2011, **3**, 349; (*k*) M. D. Pluth, R. G. Bergman and K. N. Raymond, *Acc. Chem. Res.*, 2009, **42**, 1650; (*l*) M. M. J. Smulders, I. A. Riddell, C. Browne and J. R. Nitschke, *Chem. Soc. Rev.*, 2013, **42**, 1728; (*m*) T. Nakamura, H. Ube and M. Shionoya, *Chem. Lett.*, 2014, **42**, 328; (*n*) H. Li, Z.-J. Yao, D. Liu and G.-X. Jin, *Coord. Chem. Rev.*, 2015, **293–294**, 139; (*o*) L. Chen, Q. Chen,

M. Wu, F. Jiang and M. Hong, *Acc. Chem. Res.*, 2015, **48**, 201; (*p*) T. R. Cook and P. J. Stang, *Chem. Rev.*, 2015, **115**, 7001; (*q*) L. Li, D. J. Fanna, N. D. Shepherd, L. F. Lindoy and F. Li, *J. Inclusion Phenom. Macrocyclic Chem.*, 2015, **82**, 3.

2 M. D. Ward and P. R. Raithby, *Chem. Soc. Rev.*, 2013, **42**, 1619.

3 (*a*) J. W. Yi, N. P. E. Barry, M. A. Furrer, O. Zava, P. J. Dyson, B. Therrien and B. H. Kim, *Bioconjugate Chem.*, 2012, **23**, 461; (*b*) B. Therrien, *Chem.–Eur. J.*, 2013, **19**, 8378; (*c*) J. E. M. Lewis, E. L. Gavey, S. A. Cameron and J. D. Crowley, *Chem. Sci.*, 2012, **3**, 778; (*d*) W. Cullen, S. Turega, C. A. Hunter and M. D. Ward, *Chem. Sci.*, 2015, **6**, 625.

4 (*a*) C. J. Brown, R. G. Bergman and K. N. Raymond, *J. Am. Chem. Soc.*, 2009, **131**, 17530; (*b*) C. J. Hastings, M. D. Pluth, R. G. Bergman and K. N. Raymond, *J. Am. Chem. Soc.*, 2010, **132**, 6938; (*c*) J. L. Bolliger, A. M. Belenguer and J. R. Nitschke, *Angew. Chem., Int. Ed.*, 2013, **52**, 7958; (*d*) H. Vardhan and F. Verpoort, *Adv. Synth. Catal.*, 2015, **357**, 1351; (*e*) X. Jing, C. He, Y. Yang and C. Duan, *J. Am. Chem. Soc.*, 2015, **137**, 3967; (*f*) C. García-Simón, R. Gramage-Doria, S. Raoufmoghaddam, T. Parella, M. Costas, X. Ribas and J. N. H. Reek, *J. Am. Chem. Soc.*, 2015, **137**, 2680; (*g*) C. J. Brown, F. D. Toste, R. G. Bergman and K. N. Raymond, *Chem. Rev.*, 2015, **115**, 3012.

5 (*a*) O. Chepelin, J. Ujma, X. Wu, A. M. Z. Slawin, M. B. Pitak, S. J. Coles, J. Michel, A. C. Jones, P. E. Barran and P. J. Lusby, *J. Am. Chem. Soc.*, 2012, **134**, 19334; (*b*) K. Yamashita, M. Kawano and M. Fujita, *Chem. Commun.*, 2007, 4102; (*c*) Z. Li, N. Kishi, K. Hasegawa, M. Akita and M. Yoshizawa, *Chem. Commun.*, 2011, **47**, 8605; (*d*) X. Yan, T. R. Cook, P. Wang, F. Huang and P. J. Stang, *Nat. Chem.*, 2015, **7**, 342; (*e*) L.-L. Yan, C.-H. Tan, G.-L. Zhang, L.-P. Zhou, J.-C. Bünzli and Q.-F. Sun, *J. Am. Chem. Soc.*, 2015, **137**, 8550; (*f*) C. He, Z. Lin, C. Duan, C. Xu, Z. Wang and C. Yan, *Angew. Chem., Int. Ed.*, 2008, **47**, 877; (*g*) P. D. Frischmann, V. Kinz and F. Würthner, *Angew. Chem., Int. Ed.*, 2015, **54**, 7285; (*h*) P. P. Neelakandan, A. Jiménez and J. R. Nitschke, *Chem. Sci.*, 2015, **5**, 908.

6 (*a*) A. J. Metherell and M. D. Ward, *Chem. Commun.*, 2014, **50**, 6330; (*b*) A. B. Wragg, A. J. Metherell, W. Cullen and M. D. Ward, *Dalton Trans.*, 2015, **44**, 17869; (*c*) A. J. Metherell and M. D. Ward, *Chem. Commun.*, 2014, **50**, 10979; (*d*) A. J. Metherell and M. D. Ward, *Polyhedron*, 2015, **89**, 260.

7 (*a*) Y.-T. Chan, X. Li, J. Yu, G. A. Carri, C. N. Moorefield, G. R. Newkome and C. Wesdemiotis, *J. Am. Chem. Soc.*, 2011, **133**, 11967; (*b*) H. Sato, A. Nakao and A. Yamagishi, *New J. Chem.*, 2011, **35**, 1823; (*c*) M. M. J. Smulders, A. Jimenez and J. R. Nitschke, *Angew. Chem., Int. Ed.*, 2012, **51**, 6681; (*d*) K. Li, L.-Y. Zhang, C. Yan, M. Pan, L. Zhang and C.-Y. Su, *J. Am. Chem. Soc.*, 2014, **136**, 4456; (*e*) A. Galstyan, P. J. Sanz Miguel, K. Weise and B. Lippert, *Dalton Trans.*, 2013, **42**, 16151; (*f*) P. de Wolf, S. L. Heath and J. A. Thomas, *Chem. Commun.*, 2002, 2540; (*g*) D. M. Bassani, J.-M. Lehn, S. Serroni, F. Puntoriero and S. Campagna, *Chem.–Eur. J.*, 2003, **9**, 5936; (*h*) J. Yang, M. Bhadbhade, W. A. Donald, H. Iranmanesh, E. G. Moore, H. Yan and J. E. Beves, *Chem. Commun.*, 2015, **51**, 4465; (*i*) A. J. Metherell and M. D. Ward, *Chem. Sci.*, DOI: 10.1039/c5sc03526k.

8 (*a*) X. Sun, D. W. Johnson, D. L. Caulder, K. N. Raymond and E. H. Wong, *J. Am. Chem. Soc.*, 2001, **123**, 2752; (*b*) S. Hiraoka, Y. Sakata and M. Shionoya, *J. Am. Chem. Soc.*, 2008, **130**, 10058; (*c*) W. J. Ramsay, T. K. Ronson, J. K. Clegg and J. R. Nitschke, *Angew. Chem., Int. Ed.*, 2013, **52**, 13439; (*d*) F. E. Hahn, M. Offermann, C. SchulzeIsfort, T. Pape and R. Frohlich, *Angew. Chem., Int. Ed.*, 2008, **47**, 6794; (*e*) H.-B. Wu and Q.-M. Wang, *Angew. Chem., Int. Ed.*, 2009, **48**, 7343; (*f*) A. J. Metherell and M. D. Ward, *RSC Adv.*, 2013, **3**, 14281.

9 (*a*) I. S. Tidmarsh, T. B. Faust, H. Adams, L. P. Harding, L. Russo, W. Clegg and M. D. Ward, *J. Am. Chem. Soc.*, 2008, **130**, 15167; (*b*) S. Turega, M. Whitehead, B. R. Hall, M. F. Haddow, C. A. Hunter and M. D. Ward, *Chem. Commun.*, 2012, **48**, 2752; (*c*) S. Turega, M. Whitehead, B. R. Hall, A. J. H. M. Meijer, C. A. Hunter and M. D. Ward, *Inorg. Chem.*, 2013, **52**, 1122; (*d*) M. Whitehead, S. Turega, A. Stephenson, C. A. Hunter and M. D. Ward, *Chem. Sci.*, 2013, **4**, 2744; (*e*) S. Turega, W. Cullen, M. Whitehead, C. A. Hunter and M. D. Ward, *J. Am. Chem. Soc.*, 2014, **136**, 8475.

10 A. Stephenson and M. D. Ward, *Dalton Trans.*, 2011, **40**, 10360.

11 S. L. Dabb and N. C. Fletcher, *Dalton Trans.*, 2015, **44**, 4406.

12 (*a*) S. P. Argent, H. Adams, L. P. Harding and M. D. Ward, *Dalton Trans.*, 2006, 542; (*b*) A. M. Najar, I. S. Tidmarsh, H. Adams and M. D. Ward, *Inorg. Chem.*, 2009, **48**, 11871.

13 B. Whittle, S. R. Batten, J. C. Jeffery, L. H. Rees and M. D. Ward, *J. Chem. Soc., Dalton Trans.*, 1996, 4249.

14 (*a*) M. S. Lah and V. L. Pecoraro, *J. Am. Chem. Soc.*, 1989, **111**, 7258; (*b*) A. J. Stemmler, J. W. Kampf and V. L. Pecoraro, *Inorg. Chem.*, 1995, **34**, 2271; (*c*) A. J. Stemmler, A. Barwinski, M. J. Baldwin, V. Young and V. L. Pecoraro, *J. Am. Chem. Soc.*, 1996, **118**, 11962.

15 (*a*) C. R. K. Glasson, J. K. Clegg, J. C. McMurtrie, G. V. Meehan, L. F. Lindoy, C. A. Motti, B. Moubaraki, K. S. Murray and J. D. Cashion, *Chem. Sci.*, 2011, **2**, 540; (*b*) I. A. Riddell, T. K. Ronson and J. R. Nitschke, *Chem. Sci.*, 2015, **6**, 3533.

16 I. P. Evans, A. Spencer and G. Wilkinson, *J. Chem. Soc., Dalton Trans.*, 1973, 204.

17 S. J. Coles and P. A. Gale, *Chem. Sci.*, 2012, **3**, 683.

18 G. M. Sheldrick, *SADABS: A program for absorption correction with the Siemens SMART system*, University of Göttingen, Germany, 2008.

19 G. M. Sheldrick, *Acta Crystallogr., Sect. A: Found. Crystallogr.*, 2008, **64**, 112.

20 (*a*) A. Spek, *J. Appl. Crystallogr.*, 2003, **36**, 7; (*b*) P. van der Sluis and A. L. Spek, *Acta Crystallogr., Sect. A: Found. Crystallogr.*, 1990, **46**, 194.

